

SUPERCELL EVOLUTION IN ENVIRONMENTS WITH UNUSUAL HODOGRAPHS

David O. Blanchard\* and Brian A. Klimowski  
National Weather Service, Flagstaff, Arizona

1. INTRODUCTION

The events that transpired across northern Arizona during the afternoon of 14 August 2003 resulted in an unusual severe weather episode. Although it was in the middle of the warm season North American Monsoon (NAM), which is typically dominated by high pressure over Mexico and the southwest United States, a continental low pressure system approached from the east and moved westward toward Arizona.

The combination of enhanced deep layer shear associated with the cyclone, and the ever-present deep moisture and instability associated with the NAM, produced widespread strong thunderstorms and a few long-lived supercells. Reports of damaging large hail and funnel clouds were received at the Flagstaff National Weather Service (NWS) office during the day. Radar data indicated the possibility of tornadic supercells although confirming reports were not available.

An examination of the winds aloft and the hodograph indicated that the hodograph shape retained the anticyclonic (i.e., clockwise) curvature typically associated with midwestern severe weather hodographs. On the other hand, the hodograph was rotated clockwise approximately 135° from the canonical hodographs. The mean wind and deep layer shear associated with this profile resulted in storms moving towards the southwest with right moving supercells attaining a more westerly heading, and left movers headed towards the south. Hook echoes associated with these storms were generally noted to reside on the northwestern flanks.

Our main focus in this study is to examine the vertical structure of the wind field through the use of hodographs and to make some inferences on the development of supercellular convection under these unusual wind regimes.

2. EVOLUTION OF THE LOW PRESSURE

The low pressure system that moved across Arizona had its origins over the midwestern United States several days earlier. Strong high pressure over the western United States steered the low pressure system slowly to the south towards the Gulf of Mexico and then westward

across New Mexico and Arizona (Fig. 1). With its origins in the weakly baroclinic westerlies, the thermal structure of this system remained “cold core,” rather than having the characteristics of the more typical tropical lows that move across Mexico and northward into Arizona. This thermal structure resulted in more convective instability than is often observed in these regions.



Figure 1. 500-mb location of the migrating low pressure system at 0000 UTC each day during the period 13-15 August 2004.

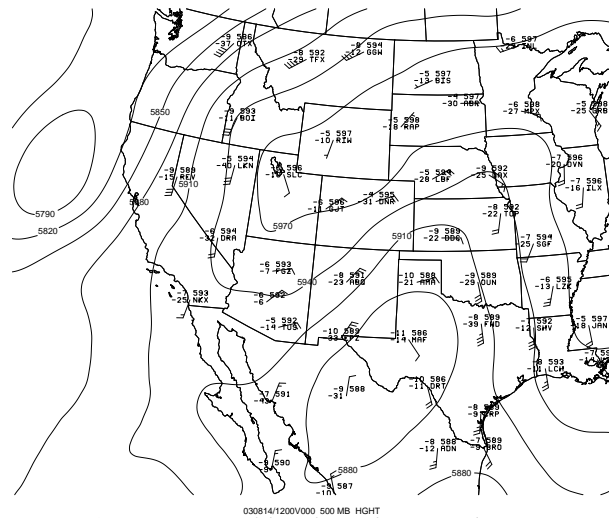


Figure 2. Geopotential height and station data at 500 mb for 1200 UTC 14 August 2004. Height contours every 30 m. Station data plotted using standard conventions.

\*Corresponding author address: David O. Blanchard, NOAA/NWS, P.O. Box 16057, Belmont, AZ 86015; email: David.O.Blanchard@noaa.gov.

Figure 2 is a depiction of the height field at 500 mb at 1200 UTC 14 August 2003. The center of the low pressure system was located along the Texas-Mexico border with minimum heights of 586 dam. Northward of this low was a high pressure ridge sprawling from southeastern California to the Great Lakes region, with maximum heights of 598 dam. A narrow band of stronger winds was located between these two features aligned from southeastern Colorado, across northwestern New Mexico, and then across east-central Arizona.

### 3. INSTABILITY AND SHEAR PARAMETERS

#### 3.1 Sounding data

Temperature and moisture profiles are shown in the Skew T–ln p plot. (Fig. 3) These profiles show a classic “onion” shape sounding signifying it had been taken in the wake of deep convection (Fig. 3a). However, with the approach of the low pressure system from the east, the sounding underwent drying aloft, moistening in the lower levels, and a steepening of the lapse rate in response to the cool pool aloft (Fig. 3b). The wind profile shows both veering of the winds with height and moderate shear through a deep layer, characteristics not typically found in a summertime sounding in this location.

Stability parameters for the 1200 UTC sounding indicate a mean layer CAPE (MLCAPE) of  $195 \text{ J kg}^{-1}$  with convective inhibition (CIN) of  $150 \text{ J kg}^{-1}$ . Surface-based CAPE (SBCAPE) was  $815 \text{ J kg}^{-1}$  with CIN of  $130 \text{ J kg}^{-1}$ . At 0000 UTC, the MLCAPE had increased to  $945 \text{ J kg}^{-1}$  with CIN of  $135 \text{ J kg}^{-1}$ ; SBCAPE was  $2185 \text{ J kg}^{-1}$  with no CIN.

The energy–helicity index (EHI; Hart and Korotky 1991; Davies 1993) is defined as

$$\text{EHI} = \frac{(\text{CAPE})(\text{SRH})}{1.6 \times 10^5}$$

This index is used operationally for supercell and tornado forecasting, with values larger than 1.0 indicating a potential for supercells, and  $\text{EHI} > 2.0$  indicating a large probability of supercells. The EHI for the 1200 UTC soundings were quite small owing to small values of CAPE. By 0000 UTC, the EHI for a surface-based parcel had increased to 2.4.

The vorticity generation parameter (VGP; Rasmussen and Blanchard 1998, hereafter RB98) is derived from an examination of the parameter space investigated in Rasmussen and Wilhelmson (1983) and the physical concept of tilting of vorticity. The rate of conversion of horizontal to vertical vorticity through tilting

can be parameterized as

$$\text{VGP} = \left[ S(\text{CAPE})^{1/2} \right]$$

Here,  $S$  is mean shear (or hodograph length divided by depth), given by

$$\bar{S} = \frac{\int_0^h V dz}{\int_0^h dz}$$

VGP was small at 1200 UTC owing to the low values of CAPE but increased to 0.31 by 0000 UTC.

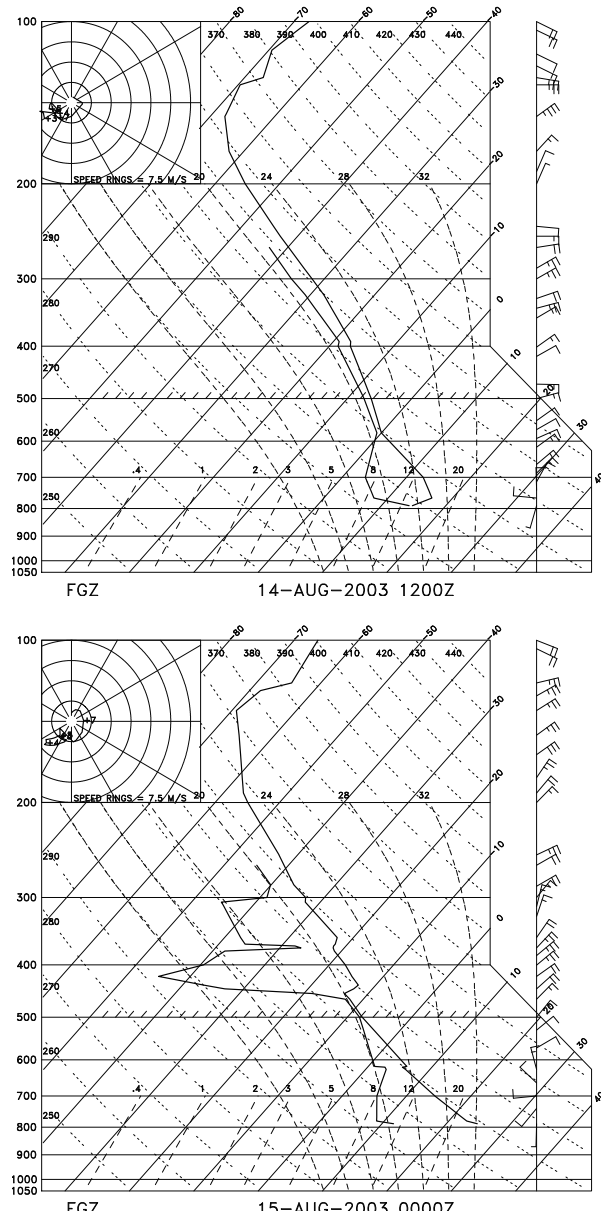


Figure 3. Skew T–ln p profile taken at Flagstaff, Arizona (KFGZ) at a) 1200 UTC 14 August, and b) 0000 UTC 15 August.

### 3.2 Model data

Grid point data from the Eta model was used to analyze additional features of the wind field and vertical instability associated with this system. Figure 4 shows the deep-layer shear (approximately the 0.5–6 km layer). There is a region with bulk shear greater than  $25 \text{ m s}^{-1}$  in the Four Corners region, with an extensive region of greater than  $20 \text{ m s}^{-1}$  shear.

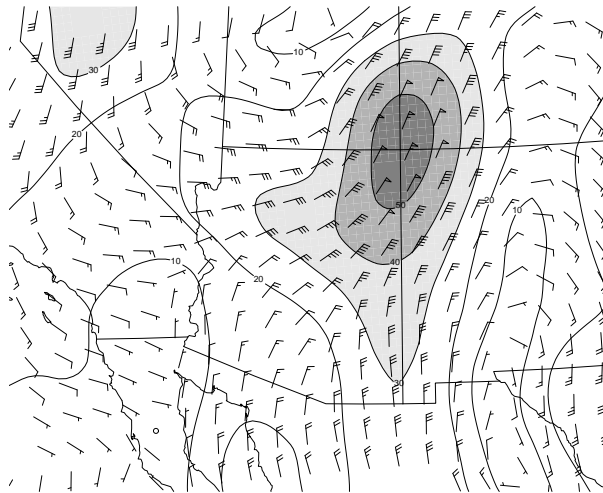


Figure 4. Deep-layer shear between 750 and 400 mb (approximately the 0.5–6 km layer). Contours every  $5 \text{ m s}^{-1}$ ; gray fill pattern at  $15$ ,  $20$ , and  $25 \text{ m s}^{-1}$ .

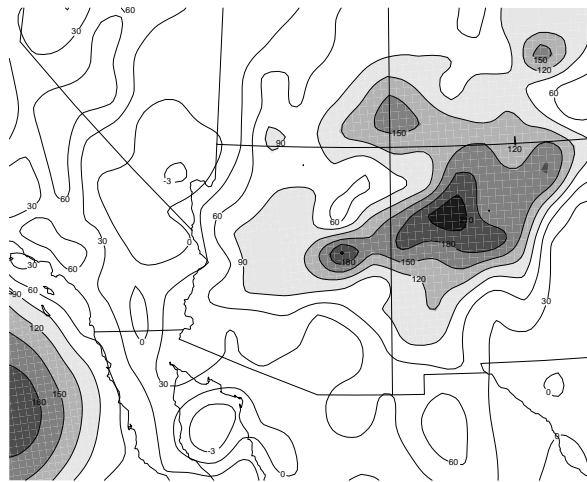


Figure 5. Storm relative helicity (SRH) at 1800 UTC 14 August 2004. Contours every  $30 \text{ m}^2 \text{ s}^{-2}$ ; gray fill starting at  $90 \text{ m}^2 \text{ s}^{-2}$ .

Figure 6 is an idealized schematic of a hodograph with anticyclonic curvature. This hodograph is rotated in the clockwise direction from the canonical hodograph typically found in midwestern supercell environments. In the right-hand half of the figure is a schematic representation of a radar depiction of a supercell rotated

clockwise the same amount. Note that this rotation results in the “hook echo” portion of the storm being located in the northern portion of the storm.

Eta model data of the 0–3 km storm-relative helicity ( $\text{SRH}_{0-3}$ ; Davies-Jones 1984, Davies-Jones et al 1990) indicated a broad band of higher values oriented from the northeast to the southwest from northwestern New Mexico across east-central Arizona (Fig. 5). Peak values were generally  $150\text{--}200 \text{ m}^2 \text{ s}^{-2}$ . Best CAPE also occurred in a broad band with the same orientation and peak values were generally  $1000\text{--}1200 \text{ J kg}^{-1}$ .

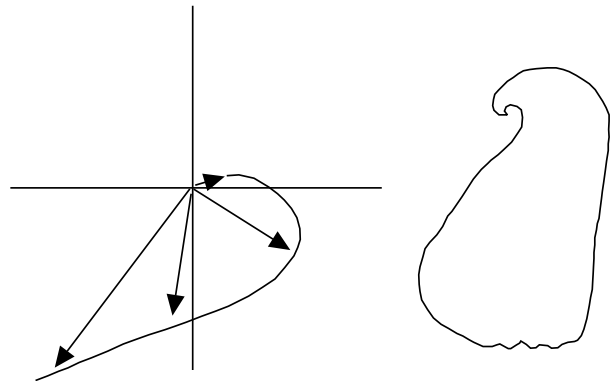


Figure 6. Idealized schematic of a hodograph typical of supercell environments (left) and a schematic representation of a radar depiction of a supercell (right). Both schematics are rotated clockwise approximately  $135^\circ$  from the canonical orientation.

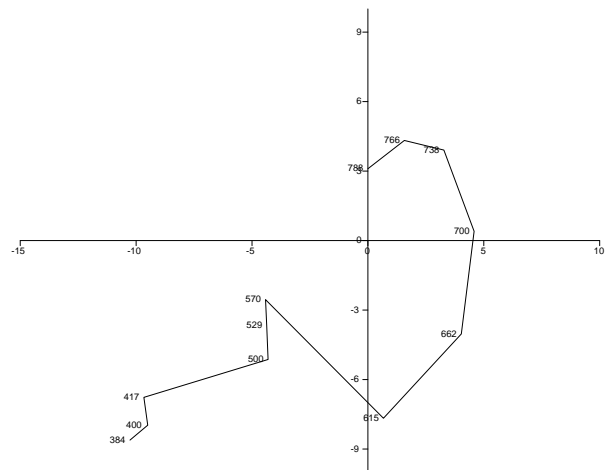


Figure 7. Hodograph from gridded model data valid 0000 UTC 15 August 2004 for a location in east-central Arizona.

Figure 7 is a model-derived hodograph from east-central Arizona for the late afternoon period (0000 UTC 15 August). This hodograph closely approximates the idealized hodograph in the left-hand side of Fig. 6. Storm motion from this hodograph would be to the southwest ( $050^\circ$  at  $10 \text{ m s}^{-1}$ ) and the hook echo would

be located in the right-rear quadrant of this storm. Once the supercell begins to deviate to the right, its motion would be more westerly ( $085^\circ$  at  $10 \text{ m s}^{-1}$ ; RB98, Bunkers et al 2000). Animations of radar imagery confirmed this and showed most storms moving to the southwest with right-moving supercells heading towards the west, and a few left-moving supercells moved towards the south.

### 3.3 Discussion of stability and shear parameters

Table 1 compares the sounding and model shear and instability parameters for this case with those discussed by RB98. In their study of convection, they analyzed shear and instability parameters associated with the environments of ordinary cells (ORD), supercells (SUP), and tornadic supercells (TOR). The results for this case indicate that at least some of the parameters compare favorably with those analyzed by RB98 for the SUP and TOR categories

*Table 1: Shear and instability parameters for 1200 and 0000 UTC soundings. Subscripts refer to the depth in kilometers above the ground through which the calculation is performed. Q-values in parenthesis refer to the quartile to which these numbers compare with the results presented in Rasmussen and Blanchard (1998).*

Parameter	1200 UTC	0000 UTC
$\text{SRH}_{0-3} \text{ (m}^2 \text{ s}^{-2}\text{)}$	155 (Q3)	175 (Q3)
$\text{CAPE (J kg}^{-1}\text{)}$	815 (Q2)	2185 (Q4)
$\text{Mean Shear}_{0-4} \text{ (x}10^{-3} \text{ s}^{-1}\text{)}$	6.9 (Q2)	6.7 (Q2)
$\text{Bulk shear}_{0.5-6} \text{ (m s}^{-1}\text{)}$	9 (Q1)	15 (Q2)
EHI	0.8 (Qx3)	2.4 (Q4)
VGP ( $\text{m s}^{-2}$ )	0.2 (Q2)	0.3 (Q3)

## 5. RADAR ANALYSIS

Animations of radar imagery from this day showed storms were moving from the northeast to the southwest. As a few of the stronger storms acquired supercell tendencies, motion deviated to the right and storm motion was to the west; left moving supercells moved towards the south. Figure 8a shows the reflectivity field from a well-developed supercell at 2353 UTC. There is a hook echo located on the northwestern flank of the westward-moving storm. Figure 8b shows the velocity field; there is a well-defined velocity couplet at the same location as the hook echo. Other storms that developed on this day exhibited these same characteristics; i.e., a hook echo on the north side of the storm as the supercell tracked to the west.

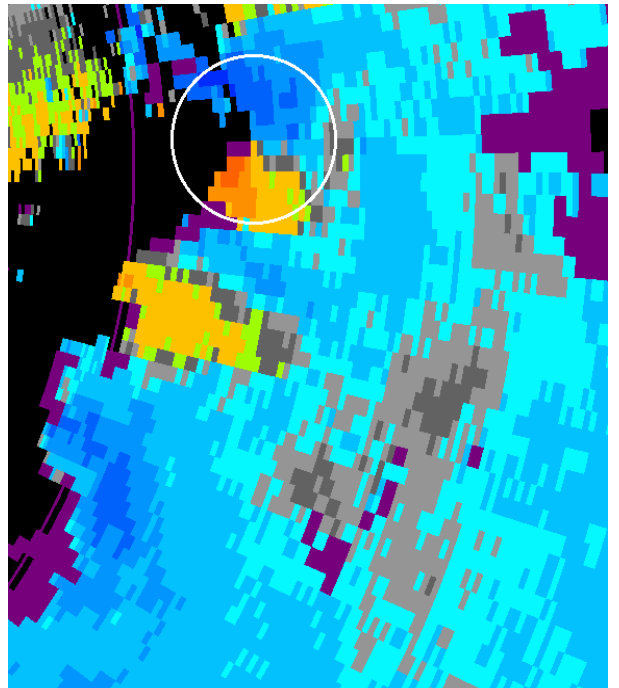
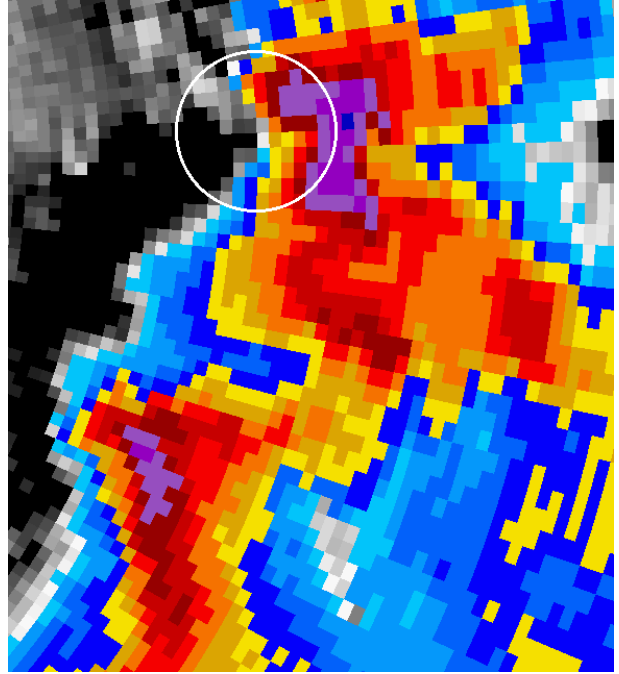


*Figure 8. Radar images from the KFSX radar at 2358 UTC 14 August showing a) reflectivity and b) velocity. The reflectivity hook echo and the velocity couplet are indicated by the circles.*

## 6. DISCUSSION

By conducting a careful examination of the winds aloft and the shape of the hodograph, an educated assessment of potential supercell evolution can be accomplished prior to the development of convection and su-

percells. Too often, forecasters expect supercells to attain the “classic” appearance, even though this can only occur with the proper curvature and orientation of the hodograph. By properly determining, in advance, the most likely shape and orientation of the supercell, the radar meteorologist can focus attention on the relevant portion of the storm looking for structures such as rotation aloft, hook echoes, and weak echo region in the appropriate quadrant of the storm. This severe weather outbreak served as an interesting example of a “non-classical” environment that led to “rotated” supercells producing large hail, funnel clouds, and, possibly, tornadoes.

## REFERENCES

- Bunkers, M. J., B. A. Klimowski, J. W. Zeitle, R. L. Thompson., and M. L. Weisman, 2000: Predicting supercell motion using a new hodograph technique. *Wea Forecasting*, **15**, 61–79.
- Davies, J. M., 1993: Hourly helicity, instability, and EHI in forecasting supercell tornadoes. Preprints, *17th Conf. on Severe Local Storms*, St. Louis, MO, Amer. Meteor. Soc., 107–111.
- Davies-Jones, R. P., 1984: Streamwise vorticity: The origin of updraft rotation in supercell storms. *J. Atmos. Sci.*, **41**, 2991–3006.
- , D. Burgess, and M. Foster, 1990: Test of helicity as a tornado forecast parameter. Preprints, *16th Conf. on Severe Local Storms*, Kananaskis Park, AB, Canada, Amer. Meteor. Soc., 588–592.
- Hart, J. A., and W. Korotky, 1991: The SHARP workstation v1.50 users guide. National Weather Service, NOAA, US. Dept. of Commerce, 30 pp. [Available from NWS Eastern Region Headquarters, 630 Johnson Ave., Bohemia, NY 11716.]
- Rasmussen, E. N., and D. O. Blanchard, 1998: A baseline climatology of sounding-derived supercell and tornado forecast parameters. *Wea. Forecasting*, **13**, 1148–1164.
- , and R. B. Wilhelmson, 1983: Relationships between storm characteristics and 1200 GMT hodographs, lowlevel shear, and stability. Preprints, *13th Conf. on Severe Local Storms*, Tulsa, OK, Amer. Meteor. Soc., J5–J8.